Inorganic Chemistry

Article

pubs.acs.org/IC

Synthesis, Crystal Structures, Magnetic Properties and Catecholase Activity of Double Phenoxido-Bridged Penta-Coordinated Dinuclear Nickel(II) Complexes Derived from Reduced Schiff-Base Ligands: Mechanistic Inference of Catecholase Activity

Apurba Biswas,[†] Lakshmi Kanta Das,[†] Michael G. B. Drew,[‡] Guillem Aromí,[§] Patrick Gamez,*[,§,∥] and Ashutosh Ghosh*[,†]

[†]Department of Chemistry, University College of Science, University of Calcutta, 92 APC Road, Kolkata 700 009, India

[‡]School of Chemistry, The University of Reading, P.O BOX 224, Whiteknights, Reading RG 66AD, United Kingdom

[§]Departament de Química Inorgànica, Universitat de Barcelona, Martí i Franquès 1-11, 08028 Barcelona, Spain

[∥]Institució Catalana de Recerca i Estudis Avançats (ICREA), Passeig Lluís Companys, 23, 08010 Barcelona, Spain

Supporting Information

ABSTRACT: Three double phenoxido-bridged dinuclear nickel(II) complexes, namely $[Ni_2(L^1)_2(NCS)_2]$ (**1**), $[Ni_2(L^2)_2(NCS)_2]$ (**2**), and $[Ni_2(L^3)_2(NCS)_2]$ (**3**) have been synthesized using the reduced tridentate Schiff-base ligands 2-[1-(3-methylamino-propylamino)-ethyl]-phenol (HL^1), 2-[1-(2-dimethylamino-ethylamino)-ethyl]-phenol (HL^2), and 2-[1-(3-dimethylamino-propylamino)-ethyl]-phenol (HL^3), respectively. The coordination compounds have been characterized by X-ray structural analyses, magnetic-susceptibility measurements, and various spectroscopic methods. In all complexes, the nickel(II) ions are penta-coordinated in a square-pyramidal environment, which is severely distorted in the case of **1** (Addison parameter $\tau = 0.47$) and **3** ($\tau = 0.29$), while it is almost perfect for **2** ($\tau = 0.03$). This arrangement leads to relatively strong antiferromagnetic interactions between the Ni(II) ($S = 1$) metal centers as mediated by double phenoxido bridges (with J values of −23.32 (**1**), −35.45 (**2**), and −34.02 (**3**) cm^3 K mol^{-1}, in the convention $H = -2JS_1S_2$). The catalytic activity of these Ni compounds has been investigated for the aerial oxidation of 3,5-di-*tert*-butylcatechol. Kinetic data analysis following Michaelis−Menten treatment reveals that the catecholase activity of the complexes is influenced by the flexibility of the ligand and also by the geometry around the metal ion. Electrospray ionization mass spectroscopy (ESI-MS) studies (in the positive mode) have been performed for all the coordination compounds in the presence of 3,5-DTBC to characterize potential complex−substrate intermediates. The mass-spectrometry data, corroborated by electron paramagnetic resonance (EPR) measurements, suggest that the metal centers are involved in the catecholase activity exhibited by the complexes.

INTRODUCTION

Transition-metal ions play important roles in living systems.[1] Accordingly, enzymes that are capable of processing molecular oxygen at ambient conditions have received a great deal of attention in the past decades,[2−4] because complexes modeling their active site may serve as efficient, mild catalysts to carry out synthetic transformations of industrial importance.[5,6] Hence, model coordination compounds for metalloenzymes with oxidase (oxygenase) activity are of particular interest for the development of bioinspired catalysts for oxidation reactions.[7] In that context, the type-3 dicopper enzyme catechol oxidase uses atmospheric dioxygen to achieve the selective oxidation of catechols to *ortho*-quinones.[8]

A variety of dinuclear copper-containing functional models of this metalloenzyme have been developed during the past 15 years,[9−11] and a number of manganese(II/III) complexes exhibiting catecholase-like activity have also been reported since the mid-2000s.[12−14] Recent investigations have shown that dinuclear nickel(II) species may mediate such catechol oxidation.[15−18] The extensive studies performed with copper-based model complexes have shown that various structural factors may affect their catalytic activity, namely the metal−metal distance, type of exogenous bridging ligand, coordination geometry around the metal ion, and flexibility of the ligand.[9] Among potential flexible ligands, reduced Schiff-base ligands have been gaining popularity over the past few years, as a result of their increased flexibility (facilitated by —CH_2—NH— moieties) compared to that of the corresponding Schiff bases, which include rigid azomethine (—CH═N—) fragments.[11,19−23] Thus, tridentate reduced Schiff bases, containing N,N,O donors, have been used to generate mostly copper(II) complexes mimicking the active site of catechol oxidase.[11]

It has been shown that phenoxido-bridged di-nickel(II) complexes may serve to mimic dinuclear biological active sites

Received: December 22, 2011
Published: July 3, 2012

   dx.doi.org/10.1021/ic202748m | *Inorg. Chem.* 2012, 51, 7993−8001

efficiently.[24] For instance, phenoxido-bridged dinuclear nickel(II) compounds have been developed that are capable of oxidizing 3,5-di-*tert*-butylcatechol (3,5-DTBC) to 3,5-di-*tert*-butylquinone (3,5-DTBQ), with rate-constant (i.e. k_{cat}) values of up to 3.24×10^4 h^{-1}.[18,25]

In the present study, reduced Schiff-base ligands with an N,N,O-donor set and containing a phenol group have been used to prepare dinuclear nickel(II) complexes, and their eventual catechol oxidase-like activity has been examined and compared subsequently. Hence, the syntheses, single-crystal X-ray structures, magnetic properties, and catecholase activity of three double phenoxido bridged dinuclear nickel(II) complexes, namely $[Ni_2(L^1)_2(NCS)_2]$ (**1**), $[Ni_2(L^2)_2(NCS)_2]$ (**2**), and $[Ni_2(L^3)_2(NCS)_2]$ (**3**), respectively obtained from the reduced Schiff-base ligands 2-[1-(3-methylamino-propylamino)-ethyl]-phenol (HL^1), 2-[1-(2-dimethylamino-ethylamino)-ethyl]-phenol (HL^2), and 2-[1-(3-dimethylamino-propylamino)-ethyl]-phenol (HL^3) are described herein. All five-coordinate nickel(II) complexes show catecholase-like activity that is most likely associated with the reduction of nickel(II) to nickel(I), as proposed for the copper-based models of this biocatalyst.

EXPERIMENTAL SECTION

Materials. All chemicals were used as commercially obtained without further purification.

Synthesis of the Reduced Schiff-Base Ligands 2-[1-(3-methylamino-propylamino)-ethyl]-phenol (HL^1), 2-[1-(2-dimethylamino-ethylamino)-ethyl]-phenol (HL^2), and 2-[1-(3-dimethylamino-propylamino)-ethyl]-phenol (HL^3). HL^1 was synthesized by refluxing a solution of 2-hydroxyacetophenone (0.60 mL, 5 mmol) and *N*-methyl-1,3-propanediamine (0.52 mL, 5 mmol) in methanol (30 mL) for 1 h.[26] The methanolic solution was subsequently cooled to 0 °C, and solid sodium borohydride (210 mg, 6 mmol) was added slowly with constant stirring. After completion of the addition, the resulting reaction mixture was acidified with concentrated HCl (5 mL) and then evaporated to dryness.[20] The reduced Schiff-base ligand HL^1 was extracted from the solid residue with methanol; the methanolic solution obtained (ca. 20 mL) was used for preparation of the coordination compounds. HL^2 and HL^3 were synthesized following the same procedure using respectively *N*,*N*-dimethylethylenediamine (0.54 mL, 5 mmol) and *N*,*N*-dimethyl-1,3-propanediamine (0.63 mL, 5 mmol).

Synthesis of Complexes 1, 2, and 3. A methanolic solution of HL^1 prepared as described above was added to a solution of $Ni(SCN)_2{\cdot}4H_2O$ (1.240 g, 5.00 mmol) in methanol (20 mL). After standing overnight in air, green single crystals of **1** suitable for X-ray diffraction were obtained. Complexes **2** and **3** were synthesized applying the same procedure, using HL^2 and HL^3, respectively. Green single crystals of **2** and **3** suitable for X-ray diffraction were obtained by slow evaporation of the solvent after one day.

Complex 1: Yield: 1.231 g (76%). $C_{26}H_{38}N_6Ni_2O_2S_2$(648.14) calcd: C, 48.18; H, 5.91; N, 12.97. Found: C, 48.29; H, 5.99; N, 12.83. IR (KBr): ν(N−H), 3253 cm^{-1}, ν(C−N), 1595 cm^{-1}; λ_{max}(nm), [ε_{max}(dm^3 mol^{-1} cm^{-1})] (acetonitrile), 656 (70), 961(35).

Complex 2: Yield: 1.116 g (72%). $C_{26}H_{38}N_6Ni_2O_2S_2$ (648.14) calcd: C, 48.18; H, 5.91; N, 12.97. Found: C, 48.02; H, 6.13; N, 12.90. IR (KBr): ν(N−H), 3265 cm^{-1}, ν(C−N), 1592 cm^{-1}; λ_{max}(nm), [ε_{max}(dm^3 mol^{-1} cm^{-1})] (acetonitrile), 638(54), 960(41).

Complex 3: Yield: 1.250 g (74%). $C_{28}H_{42}N_6Ni_2O_2S_2$ (676.20) calcd: C, 49.73; H, 6.26; N, 12.43. Found: C, 49.86; H, 6.33; N, 12.28. IR (KBr): ν(N−H), 3178 cm^{-1}, ν(C−N), 1594 cm^{-1}; λ_{max}(nm), [ε_{max}(dm^3 mol^{-1} cm^{-1})] (acetonitrile), 676(37), 962(24).

Catalytic Oxidation of 3,5-DTBC. 100 equiv of 3,5-di-*tert*-butylcatechol (3,5-DTBC) in acetonitrile were added to 10^{-4} M solutions of **1**, **2**, and **3** in acetonitrile under aerobic condition at room temperature. Absorbance vs wavelength (wavelength scan) plots were generated for these reaction mixtures, recording spectrophotometric data at a regular time intervals of 10 min in the range 300−600 nm. To determine the substrate concentration dependence of the rate and to determine various kinetic parameters, 10^{-4} M solutions of the different complexes were treated with 10, 30, 50, 70, and 100 equivalents of substrate. The reactions were followed spectrophotometrically by monitoring the increase in absorbance at 400 nm (corresponding to the quinone band maxima) as a function of time (time scan).

Physical Measurements. Elemental analyses (C, H, and N) were performed using a Perkin-Elmer 240C elemental analyzer. IR spectra of KBr pellets (4500−500 cm^{-1}) were recorded using a Perkin-Elmer RXI Fourier transform infrared (FT-IR) spectrophotometer. Electronic spectra in acetonitrile (1200−300 nm) were recorded on a Hitachi U-3501 spectrophotometer. Electrochemical studies were performed with a PAR 273 potentiostat. The measurements were done at 300 K with10^{-3} M deoxygenated (through nitrogen bubbling) acetonitrile solutions of the complexes, containing 0.2 M TEAP. The working, counter, and reference electrodes used were respectively a platinum wire, a platinum coil, and an SCE (saturated calomel electrode). Electrospray ionization mass (ESI-MS positive) spectra were recorded on a MICROMASS Q-TOF mass spectrometer. Electron paramagnetic resonance (EPR) experiments were performed at liquid-nitrogen temperature (77 K) in acetonitrile, using a Bruker EMX-X band spectrometer. Variable-temperature magnetic-susceptibility data were obtained with a Quantum Design MPMS5 SQUID magnetometer. Pascal's constants were utilized to estimate diamagnetic corrections to the molar paramagnetic susceptibility.[27]

Crystal Data Collection and Refinement. Crystal data for the three coordination compounds are given in Table 1. 4003, 4209 independent reflection data were collected for **1** and **2**, with Mo Kα radiation at 150 K using an Oxford Diffraction X-Calibur charge coupled device (CCD) system. The single crystals were positioned at 50 mm from the CCD. 321 frames were measured with a counting time of 10 s. Data analyses were carried out with the CrysAlis[28] program. 2758 independent reflection data were collected for **3**, with a graphite monochromator and Mo Kα (λ = 0.71073 Å) radiation at 296 K using a Bruker SMART diffractometer. All three structures were solved using direct methods with the Shelxs97[29] program. The non-hydrogen atoms were refined with anisotropic thermal parameters. The hydrogen atoms bonded to carbon were included in geometric positions and given thermal parameters equivalent to 1.2 times those of the atom to which they were attached. Methyl hydrogen atoms were given a factor of 1.5. Absorption corrections for **1**, and **2** were carried out using the ABSPACK program.[30] In **1**, the methyl group bonded

Table 1. Crystal Data and Structure Refinement for 1−3

	1	2	3
formula	$C_{26}H_{38}N_6Ni_2O_2S_2$	$C_{26}H_{38}N_6Ni_2O_2S_2$	$C_{28}H_{42}N_6Ni_2O_2S_2$
M	648.14	648.14	676.20
crystal system	monoclinic	monoclinic	monoclinic
space group	*P*21/*n*	*P*21/*c*	*P*21/*n*
a (Å)	9.2781(5)	7.4806(5)	8.947(5)
b (Å)	12.2358(15)	12.5065(7)	20.602(12)
c (Å)	12.7526(10)	15.5699(10)	9.435(5)
α (deg)	90	90	90
β (deg)	90.697(7)	90.052(6)	115.400(6)
γ (deg)	90	90	90
V ($Å^3$)	1447.6(2)	1456.66(16)	1571.0(15)
Z	2	2	2
D_c (g cm^{-3})	1.487	1.478	1.429
μ (mm^{-1})	1.480	1.470	1.367
F (000)	680	680	712
R(int)	0.026	0.040	0.052
total reflections	6681	10015	10657
unique reflections	4003	4209	2758
$I > 2\sigma(I)$	2544	3075	2053
*R*1, *wR*2	0.0376, 0.0818	0.0360, 0.0853	0.0483, 0.1185
temp. (K)	150	150	296

dx.doi.org/10.1021/ic202748m | *Inorg. Chem.* 2012, 51, 7993−8001

to carbon was disordered over two tetrahedral sites with occupancies of 0.61(1) and 0.39(1). The structures were refined on F^2 to $R1$ 0.0376, 0.0360, and 0.0483; $wR2$ 0.0818, 0.0853, 0.1185, for 2544, 3075, 2053 data with $I > 2\sigma(I)$, respectively.

RESULTS AND DISCUSSION

Synthesis of the Complexes. The condensation of *N*-methyl-1,3-propanediamine, *N*,*N*-dimethylethylenediamine, and *N*,*N*-dimethyl-1,3-propanediamine in 1:1 molar ratio with 2-hydroxyacetophenone afforded the Schiff bases, 2-[1-(3-methylamino-propylimino)-ethyl]-phenol, 2-[(2-dimethylamino-ethylimino)-methyl]-phenol, and 2-[1-(3-dimethylamino-propylimino)-ethyl]-phenol, respectively. *In situ* reduction with sodium borohydride readily produced the tridentate ligands HL^1, HL^2, and HL^3 (Scheme 1). Reaction of 1 equiv of nickel(II)

Scheme 1. Preparation of the Coordination Compounds

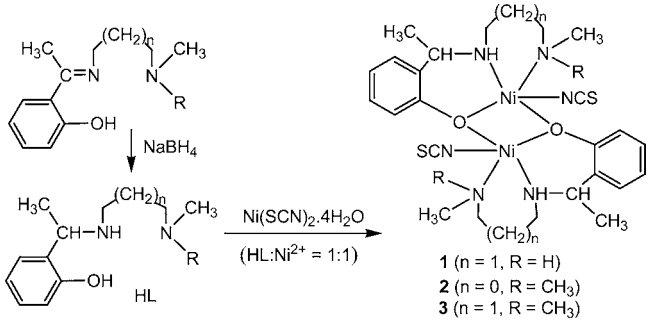

thiocyanate tetrahydrate with 1 equiv of HL^1, HL^2, and HL^3, respectively, yielded compounds **1**, **2**, and **3** (Scheme 1).

IR and Electronic Spectra. The IR spectra of complexes **1**, **2**, and **3** exhibit a moderately strong, sharp peak at respectively 3253, 3265, and 3178 cm^{-1}, which is ascribed to the N−H stretching vibration, therefore confirming that the imine group of the Schiff base has been reduced. The absence of the −C═N− moiety is corroborated further by the nonappearance of the typical strong band due to the imine vibration, which appears in the region 1620−1650 cm^{-1} for the corresponding complexes from the unreduced Schiff bases.[26,31] Absorption bands are observed at 2107, 2070, 2096 cm^{-1} for **1**, **2**, and **3**, respectively, which characterize $\nu_{C\equiv N}$ vibrations of thiocyanate anions.[32]

The electronic spectra of the three compounds, recorded in acetonitrile, show absorption bands at 656, 638, and 676 nm for **1**, **2**, and **3**, respectively, which are associated to weaker ones centered at 961, 960, and 962 nm. The electronic spectrum for a five-coordinate nickel(II) compound with a square-pyramidal geometry is expected to exhibit absorption bands near 1150 (ν_1), 950 (ν_2), and 600 nm (ν_3),[33] corresponding to the spin-allowed d−d transitions $^3A_{2g} \rightarrow {}^3T_{2g}(F)$ (ν_1), $^3A_{2g} \rightarrow {}^3T_{1g}(F)$ (ν_2) and $^3A_{2g} \rightarrow {}^3T_{1g}(P)$ (ν_3), respectively. In the present case, the ν_1 band cannot be located. The observation of the ν_2 and ν_3 bands suggest that the di-nickel(II) units are maintained in solution; actually, mass-spectrometry studies indicate that compounds **1**−**3** exist in acetonitrile solutions.

Description of the Solid-State Structures of Complexes 1, 2, and 3. All three structures are centrosymmetric dimers of nickel ions which are penta-coordinated by the three donor atoms of one ligand, the bridging phenoxido O atom from a second ligand, and a monodentate NCS^- anion. The coordination geometries vary between a highly distorted trigonal bipyramid (**1**), a square pyramid (**2**), and a distorted square pyramid (**3**).

The molecular structure of **1** is shown in Figure 1 together with its atomic-numbering scheme. Selected bond distances and

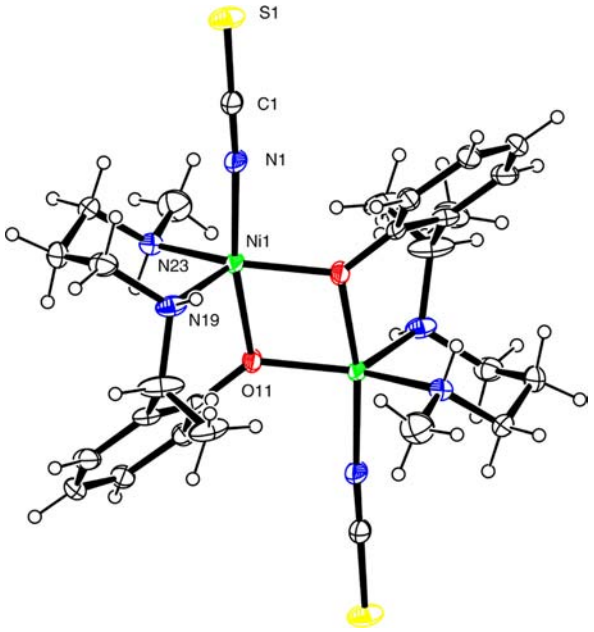

Figure 1. Illustration of the centrosymmetric structure of **1** with thermal ellipsoids at the 30% probability level.

angles are given in Table 2. The nickel atoms are five-coordinate in a trigonal-bipyramidal environment, whose axial positions are

Table 2. Selected Bond Distances (Å) and angles (deg) for 1−3[a]

	1 (x = 3)	**2** (x = 2)	**3** (x = 3)
Ni(1)−N(1)	2.0079(19)	1.9935(17)	2.012(4)
Ni(1)−O(11)	2.0205(14)	2.0167(12)	2.025(3)
Ni(1)−N(19)	2.030(2)	2.0724(16)	2.070(3)
Ni(1)−N(2x)	2.0468(17)	2.0781(16)	2.099(4)
Ni(1)−O(11)^a	1.9771(15)	2.0295(12)	2.011(3)
O(11)^a −Ni(1)−N(1)	94.78(7)	98.99(6)	98.82(14)
O(11)^a −Ni(1)−O(11)	75.46(7)	77.08(6)	76.17(11)
N(1)−Ni(1)−O(11)	169.09(8)	162.81(7)	166.86(14)
O(11)^a −Ni(1)−N(19)	123.22(7)	160.99(6)	149.61(12)
N(1)−Ni(1)−N(19)	98.01(8)	88.16(7)	88.44(15)
O(11)−Ni(1)−N(19)	91.53(7)	90.88(5)	90.14(12)
O(11)^a−Ni(1)−N(2x)	140.55(7)	111.46(6)	107.27(13)
N(1)−Ni(1)−N(2x)	93.33(7)	93.45(7)	92.07(16)
O(11)−Ni(1)−N(2x)	91.33(7)	103.59(6)	101.00(13)
N(19)−Ni(1)−N(2x)	93.59(8)	85.45(6)	101.87(14)

[a]Symmetry operation: (a = −x, −y, −z) in **1**, (a = 1 − x, 2 − y, 1 − z) in **2**, (a = −x, 2 − y, 1 − z) in **3**.

occupied by the oxygen atom O(11) from the tridentate ligand at a distance of 2.0205(14) Å, and the thiocyanate nitrogen atom N(1) at a distance of 2.0079(19) Å. The equatorial plane is characterized by the bond lengths Ni(1)−N(19) = 2.030(2), Ni(1)−N(23) = 2.0468(17), and Ni(1)−O(11)^a = 1.9771(15)Å (a = −x, −y, −z). The Ni···Ni separation distance amounts to 3.162(5) Å and the Ni(1)−O(11)−Ni(1)^a angle is 104.54(7)°. The rms deviation of the nickel center from the equatorial plane is 0.0773(2) Å. The Addison parameter (τ)[34] for the penta-coordinated nickel(II) ions in **1** is 0.47, thus indicating that the

dx.doi.org/10.1021/ic202748m | Inorg. Chem. 2012, 51, 7993−8001

Table 3. Hydrogen Bonding Distances (Å) and Angles (deg) for 1 and 3[a]

complex	D−H···A	D−H (Å)	A···H (Å)	D···A (Å)	∠D−H−A (deg)
1	N(19)−H(19)···S(1)[b]	0.91	2.55	3.454(2)	175
3	N(19)−H(19)···S(1)[c]	0.91	2.65	3.435(4)	146

[a]Symmetry operation: (b = 1 − x, −y, −z), (c = −x, 2 − y, 2 − z).

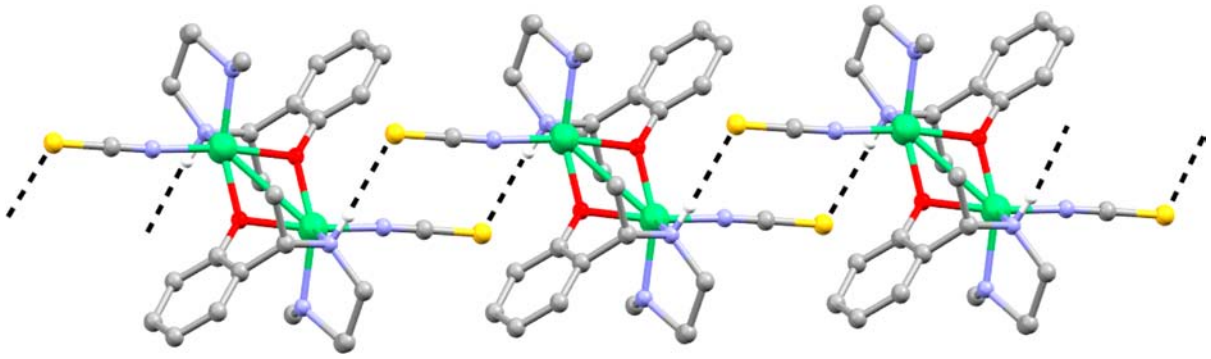

Figure 2. Hydrogen-bonding network producing a supramolecular polymer of **1**.

geometry is a significantly distorted trigonal bipyramid with N(1) and O(11) at the axial positions, forming a *trans* N(1)−Ni−O(11) angle of 169.09(8)°.

In the crystal lattice, the di-nickel units are connected by double hydrogen bonds, namely N(19)−H(19) to S(1)[b] (b = 1 − x, −y, −z) with N···S 3.454(2) Å, H···S 2.55 Å, N−H···S 175° (Table 3), giving rise to a 1-D supramolecular polymer (Figure 2).

The molecular structure of **2** is shown in Figure 3. In this compound, the deprotonated tridentate ligand 2-[1-(2-dimethyl-amino-ethylamino)-ethyl]-phenolato contains one methylene group less in the aliphatic chain between the nitrogen atoms, compared to $(L^1)^-$. However, the environment of **2** is similar to that of **1**, with a coordination geometry closer to a square pyramid (τ = 0.03) with one axial site. The basal bond lengths Ni(1)−N(19) = 2.0724(16) Å and Ni(1)−O(11)[a] (a = 1 − x, 2 − y, 1 − z) = 2.0295(12) Å are significantly longer than those found in **1**. The remaining basal distances (i.e. Ni(1)−N(1) = 1.9935(17) Å and Ni(1)−O(11) = 2.1067(12) Å) are comparable to those of **1**. The axial position is occupied by the nitrogen atom N(22) at a distance of 2.0781(16) Å. The two Ni atoms are separated by a distance of 3.165(1) Å, and the Ni(1)−O(11)−Ni(1)[a] angle amounts to 102.92(6)°. The deviations of the coordinating atoms O(11), N(1), N(19), O(11)[a] from the least-squares mean plane through them are −0.0043(13), −0.0036(15), 0.0038(15), and 0.0041(13) Å, respectively. The deviation of the nickel(II) ion from the same plane is 0.2947(2) Å in the direction of the axial N(22) atom.

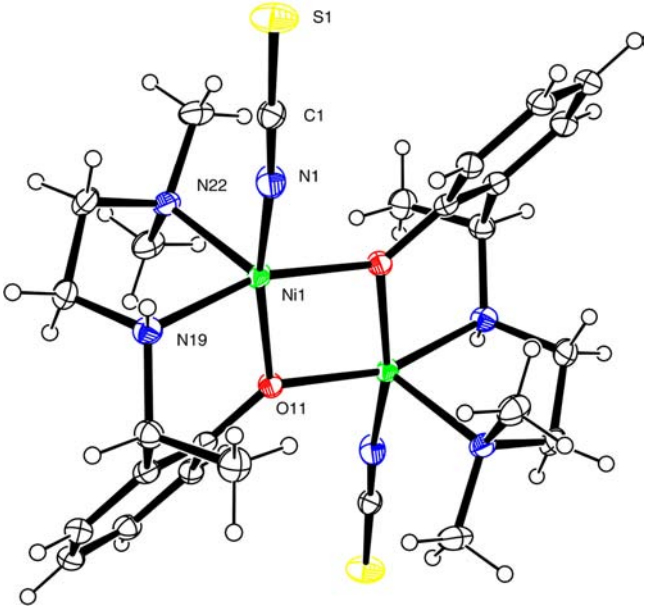

Figure 3. Illustration of the centrosymmetric structure of **2** with thermal ellipsoids at the 30% probability level.

The molecular structure of **3** is shown in Figure 4. Although $(L^3)^-$ contains three methylene groups between the two nitrogen atoms as does $(L^1)^-$ (compound **1**), the coordination geometry of **3** is closer to that of **2**. The basal plane of the distorted square pyramid (τ = 0.29) is formed by the atoms N(1), O(11), N(19), and O(11)[a] (a = −x, 2 − y, 1 − z), with bond lengths of, respectively, 2.012(4) Å, 2.025(3) Å, 2.070(3) Å, and 2.011(3) Å. The axial position is occupied by N(23) at a distance of 2.099(4) Å.

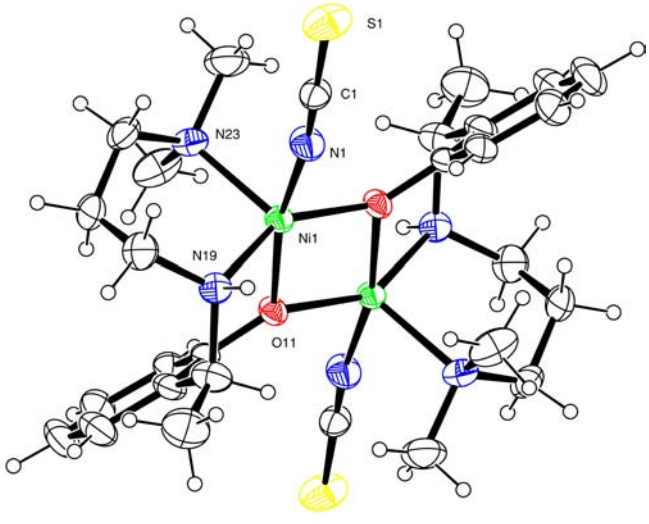

Figure 4. Illustration of the centrosymmetric structure of **3** with thermal ellipsoids at the 30% probability level.

dx.doi.org/10.1021/ic202748m | *Inorg. Chem.* 2012, 51, 7993−8001

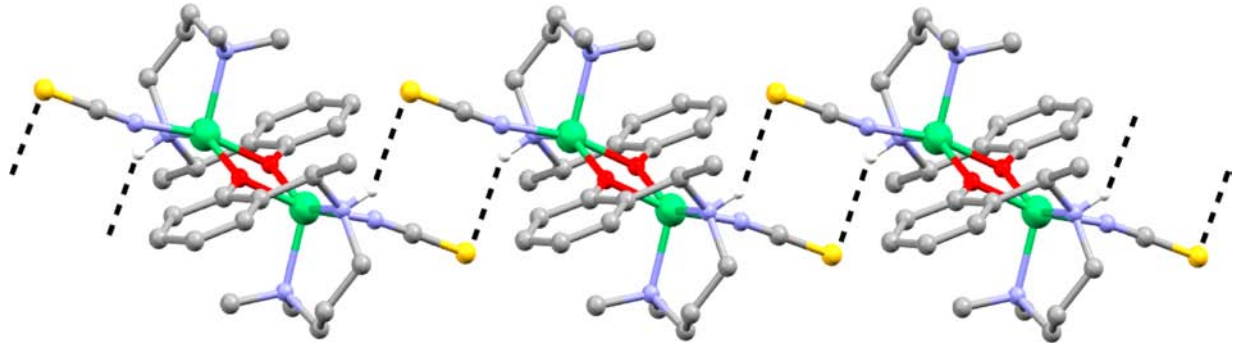

Figure 5. Hydrogen-bonding network producing a supramolecular polymer of **3**.

The two Ni atoms are separated by a distance of 3.178 (2) Å, and the Ni(1)−O(11)−Ni(1)^a angle is 103.84(12)°. The deviations of the coordinating atoms O(11), N(1), N(19), O(11)^a from the least-squares mean plane through them are 0.148(3), 0.123(4), −0.130(4), and−0.141(3) Å, respectively. The deviation of the nickel(II) ion from the same plane is 0.3639 (5) Å, in the direction of the axial atom N(23).

Similarly to **1**, the dimers of **3** are connected by double intermolecular hydrogen bonds [N(19)−H···S(1)^c ($c = -x, 2 - y, 2 - z$) = 3.435(4) Å, angle N−H···S = 146°], resulting in a 1-D supramolecular polymer (Figure 5).

Surprisingly, the amine hydrogen atom H(19) is involved in the formation of 1-D polymeric frameworks in **1** and **3**, while this is not observed in the solid-state structure of **2**. It is also worth mentioning here that most of the nickel(II) complexes from similar N,N,O-donor Schiff bases derived from ethylenediamine described in the literature are mononuclear square-planar compounds.[35,36] A number of phenoxido-bridged dinuclear complexes have been reported as well, particularly with Schiff-base ligands derived from 1,3-propanediamine. Interestingly, in these coordination compounds, an additional anionic bridge or coordinated solvent molecule is present, thus generating hexa-coordinate nickel(II) species.[26,37,38] A few penta-coordinated double phenoxido-bridged nickel(II) dimers with tetradentate or macrocyclic ligands have been described.[39] To the best of our knowledge, the present complexes represent the first report of double phenoxido-bridged penta-coordinated dinuclear nickel(II) complexes of tridentate reduced Schiff-base ligands.[40]

Magnetic Studies. Variable temperature, bulk magnetization measurements were performed on powdered microcrystalline samples of **1**, **2** and **3**, under a constant magnetic field of 7 kG, in the 2−300 K range. The results are shown in Figure 6

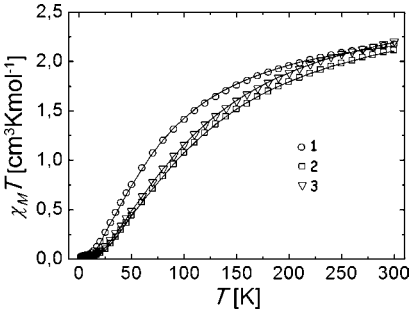

Figure 6. Plots of $\chi_M T$ vs T per mole of **1**, **2**, and **3**, respectively, from measurements collected under a constant magnetic field of 7 kG. Solid lines are best fits to the appropriate model (see text for details).

in the form of $\chi_M T$ vs T plots (where χ_M is the molar paramagnetic susceptibility). In all three cases, the behavior is very similar; a decrease of the product $\chi_M T$ takes place upon cooling, from 2.17, 2.11, and 2.20 cm^3 K mol^{-1} for **1**, **2**, and **3**, respectively, (the expected value for two nickel(II) ions with $g = 2$ is 2.00 cm^3 K mol^{-1}) to almost nil at the lowest measured temperature (reaching 0.02, 0.01, and 0.02 cm^3 K mol^{-1}, respectively, at 2 K). These results are mainly the consequence of a strong antiferromagnetic interaction between pairs of nickel(II) ions in each of the complexes, as mediated by double phenoxido bridges, which should dominate over any other effect (such as that from single ion zero field splitting or intermolecular interactions). Accordingly, the experimental data were fit to a model by use of a $\chi_M = f(T)$ expression (eq 1) obtained from the Van Vleck equation[41] as derived from the exchange Hamiltonian $H = -2JS_1S_2$ ($S_1 = S_2 = 1$), and by considering the influence of a residual fraction, ρ, of paramagnetic impurity.

$$\chi_M = (1 - \rho)\frac{Ng^2\beta^2}{kT} \times \frac{2e^{2J/kT} + 10e^{6J/kT}}{1 + 3e^{2J/kT} + 5e^{6J/kT}} + \rho\frac{2Ng^2\beta^2}{3kT} \quad (1)$$

The fits lead to the following parameters for compounds **1**, **2**, and **3**; $J = -23.32$, -35.45, and -34.02 cm^3 K mol^{-1}, $g = 2.27$, 2.35, and 2.39, and $\rho = 0.03$, 0.02, and 0.02, respectively. The results are in line with magnetostructural correlations suggesting that nickel(II) centers bridged by double alkoxido or hydroxido bridges exhibit antiferromagnetic interactions for Ni−O−Ni angles larger than 98°,[42] the coupling being more intense as the angle gets wider. The coupling here is however stronger than usually seen for phenoxido bridged nickel(II) centers.[43] In fact, the existing correlations involving two Ni−O−Ni bridges are made for the most part on compounds with six coordinate nickel(II) centers. An example very related to the present case involves a family of [Ni$_2$] complexes with penta- or hexacoordinate metal centers,[44] made with a macrocyclic ligand equivalent to two fused units of HL^1, which displays a linear correlation of J with the Ni−O−Ni angles and with the Ni−O distances.[45] The range of J values observed in such series is −17 to −67 cm^{-1}. Compounds **1**, **2**, and **3**, however, do not follow this correlation, perhaps because the macrocyclic ligand involved in those complexes imposes geometric restrains that are not present here. For example, a major difference is that the axial positions of the metals in the correlated complexes are always occupied by exogenous ligands. On the contrary, the complexes reported here exhibit always an SCN$^-$ ligand on an

dx.doi.org/10.1021/ic202748m | Inorg. Chem. 2012, 51, 7993−8001

equatorial position rather than apical. Very likely, electronic factors are at the root of the differences between the group of complexes **1** to **3** and the series of complexes previously studied.

Catecholase Activity Study and Kinetics. In most investigations dedicated to the study of the potential catecholase activity of biomimicking coordination compounds, 3,5-di-*tert*-butylcatechol (3,5-DTBC) is chosen as the model substrate. Its low redox potential makes it easy to oxidize and the bulky *tert*-butyl substituents prevent further overoxidation reactions such as ring-opening.[46] The oxidation product 3,5-di-*tert*-butylquinone (3,5-DTBQ) is highly stable and shows a maximum absorption at 403 nm in pure acetonitrile. The ability of the dinuclear complexes **1**−**3** to potentially mediate the oxidation of 3,5-DTBC was first examined. For this purpose, 10^{-4} M acetonitrile solutions of the different complexes were treated with 100 equivalents of 3,5-DTBC, under aerobic conditions. After addition of the catecholic substrate, the development of an absorption band around 400 nm is observed by UV−vis spectroscopy, which is indicative of the formation of the corresponding quinone 3,5-DTBQ. The results are shown in Figure 7 and Figures S1 and S2 in the Supporting Information for

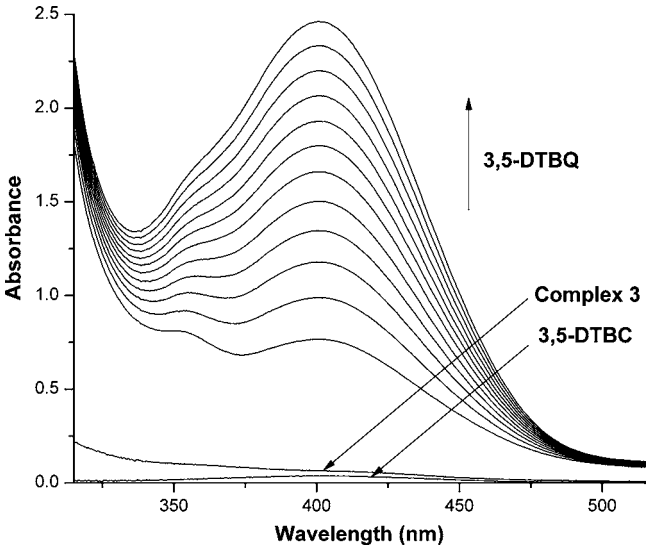

Figure 7. Increase in absorbance around 400 nm, after addition of 100 equivalents of 3,5-DTBC to a 10^{-4} M acetonitrile solution of **3**. The spectra were recorded every 10 min.

compounds **3**, **1**, and **2**, respectively. Comparison of these spectroscopic data with those obtained for the same reaction with $Ni(SCN)_2{\cdot}4H_2O$ (Figure S3, Supporting Information), which does not show catecholase activity, corroborates the capability of **1**−**3** to perform 3,5-DTBC oxidation.

Kinetic studies of the oxidation of 3,5-DTBC to 3,5-DTBQ mediated by **1**−**3** were carried out by the method of initial rates, following the absorption increase at 400 nm. The rate constant for a particular complex/substrate mixture was determined from the $\log[A_\alpha/(A_\alpha - A_t)]$ vs time plot. The substrate concentration dependence of the oxidation rate was examined under aerobic conditions, using10^{-4} M solutions of **1**, **2**, and **3** and increasing amounts of 3,5-DTBC (from 10 to 100 equiv). In all cases, first-order dependence was observed at low substrate concentrations, whereas saturation kinetics was found at higher substrate concentrations (see Figure 8 and Figures S4 and S5 in the Supporting Information for complexes **3**, **1**, and **2**, respectively). The substrate concentration dependence suggests that the initial step of the catalytic cycle is the binding of the substrate to the catalyst. Michaelis−Menten kinetics was applied to analyze the data obtained, and the Michaelis−Menten constant (K_M) and maximum initial rate (V_{max}) were determined by linearization using Lineweaver−Burk plots.[12] The turnover number (k_{cat}) values can be calculated by dividing the V_{max} values by the concentration of the corresponding complexes (Table 4). The catecholase activity follows the

Table 4. Kinetic Parameters for the Oxidation of 3,5-DTBC to 3,5-DTBQ Mediated by 1, 2, and 3 in Acetonitrile

complex	V_{max} (M min^{-1})	K_M (M)	k_{cat} (h^{-1})
1	$(10.7 \pm 0.7) \times 10^{-5}$	$(7.2 \pm 0.4) \times 10^{-3}$	64.1 ± 4.1
2	$(8.5 \pm 1.0) \times 10^{-5}$	$(7.8 \pm 0.9) \times 10^{-3}$	51.1 ± 6.2
3	$(13.6 \pm 0.8) \times 10^{-5}$	$(8.1 \pm 0.5) \times 10^{-3}$	81.7 ± 4.7

order: **3** > **1** > **2** (Figure 8 and Figures S4 and S5 in the Supporting Information, respectively).

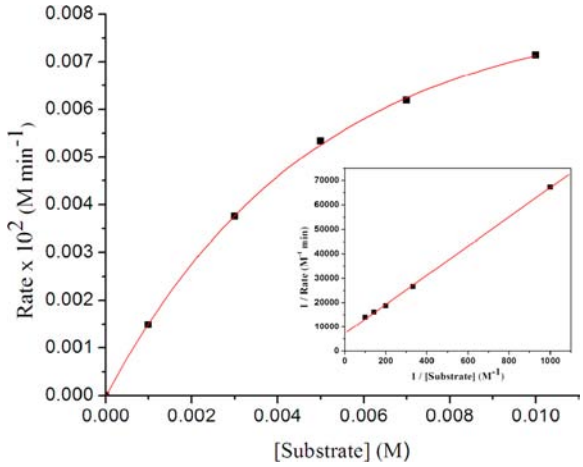

Figure 8. Plot of the initial rates versus substrate concentration for the oxidation of 3,5-DTBC catalyzed by **3**. The inset shows Lineweaver−Burk plot.

Detailed investigations with copper-based model complexes of catechol oxidase have shown that various factors may affect their catalytic activity, such as the metal−metal distance, the flexibility of the ligand, the type of exogenous bridging ligand, and the coordination geometry around the metal center.[9] Among the di-nickel compounds reported herein, the highest catecholase activity (i.e. $k_{cat} = 81.7 \pm 4.7\ h^{-1}$; Table 4) is observed for **3**. This greater catalytic activity may be attributed in part to the conformational flexibility of the chelating ligand $(L^3)^-$ facilitated by the propyl linker between the two nitrogen atoms; the flexibility of the resulting six-membered coordination ring may favor the approach and binding of the substrate to the square-pyramidal metal center(s). The lower catalytic activity exhibited by **1** ($k_{cat} = 64.1 \pm 4.1\ h^{-1}$; Table 4), whose ligand $(L^1)^-$ has a trimethylene linker as does $(L^3)^-$, may be explained by steric congestion around the highly distorted trigonal−bipyramidal environment of the nickel ions, hindering the coordination of 3,5-DTBC to the active site(s). Similarly, the lower rate constant achieved with **2** ($k_{cat} = 51.1 \pm 6.2\ h^{-1}$; Table 4) is attributable to the shorter ethyl linker that produces a more rigid five-membered coordination ring, with increased steric hindrance that most

dx.doi.org/10.1021/ic202748m | *Inorg. Chem.* 2012, 51, 7993−8001

likely impedes the approach of the catecholic substrate. Such features have also been found with copper(II) complexes.[11,48] The k_{cat} values in the range 51−82 h^{-1} obtained for complexes **1**−**3** are significantly lower than those reported so far for di-nickel(II) coordination compounds (see Table 5). However, it should be mentioned here that the k_{cat} values described in the literature were obtained with dinucleating ligands, while mononucleating ones were used in the present study. The oxidation of catechol to the corresponding quinone is a two-electron process; therefore, it requires two nickel centers that will shuttle between the +2 and +1 states. Consequently, it logically expected that a ligand that can hold two nickel ions will generate more active catalytic species. In addition, these high k_{cat} values were achieved in methanol (Table 5), while the catecholase activities of **1**−**3** were evaluated in acetonitrile; for instance, the di-nickel(II) compound $[Ni_2(LH_2)(H_2O)_2(OH)(NO_3)](NO_3)_3$, which gives a k_{cat} of 14400 h^{-1} in methanol, is inactive in acetonitrile (Table 5).[16] Compared to most dinuclear copper(II) model systems reported earlier, complexes **1**−**3** exhibit comparable k_{cat} values (Table 5). Indeed, except for the compounds $[Cu_2(H_2L2^2)(OH)(H_2O)(NO_3)](NO_3)_3{\cdot}2H_2O$[47] and $[Cu_2L1(N_3)_2{\cdot}2H_2O]$[48] that show remarkably elevated rate constants of respectively 32400 and 21600 h^{-1}, the majority of the dicopper(II) complexes described in previous studies have k_{cat} values in the range 12−900 h^{-1} (Table 5).

Table 5. Kinetic Parameters for the Oxidation of 3,5-DTBC to 3,5-DTBQ mediated by 1, 2, and 3

complex	k_{cat} (h^{-1}) in methanol	k_{cat} (h^{-1}) in acetonitrile	ref
1	n.d.[a]	64.1 ± 4.1	present work
2	n.d.[a]	51.1 ± 6.2	present work
3	n.d.[a]	81.7 ± 4.7	present work
Di-nickel(II) Compounds			
$[Ni_2(LH_2)(H_2O)_2(OH)(NO_3)](NO_3)_3$	14400	inactive	ref 16
$[Ni_2L(NO_3)(H_2O)_3]NO_3$	1500	n.d.[a]	ref 18
Dicopper(II) Compounds			
$[\{Cu_2L(\mu{-}OH)(H_2O)\}(\mu\text{-}ClO_4)]_n(ClO_4)_n$	n.d.[a]	167.9	ref 46
$[\{Cu_2L(\mu_{1,1}\text{-}N_3)(ClO_4)\}_2(\mu_{1,3}\text{-}N_3)_2]$	n.d.[a]	215.1	ref 46
$[Cu_2(H_2L2^2)(OH)(H_2O)(NO_3)](NO_3)_3{\cdot}2H_2O$	32400	n.d.[a]	ref 47
$[Cu_2L1(N_3)_2{\cdot}2H_2O]$	18000	21600	ref 48
$[Cu_2(HL^2)(O_2CPh)(H_2O)]PhCO_2{\cdot}H_2O$	26	n.d.[a]	ref 49
$[Cu_2(\mu{-}OH)(C_{21}H_{33}ON_6)](ClO_4)_2{\cdot}H_2O$	12[b]	n.d.[a]	ref 10c
$[Cu_2(BPMP)(OAc)_2][ClO_4]{\cdot}H_2O$	n.d.[a]	900	ref 50

[a]Not determined. [b]In MeOH/water (32:1, v/v).[10c]

The binding of 3,5-DTBC to the different nickel(II) complexes has been investigated by mass spectrometry (ESI; positive mode); hence, ESI-MS spectra have been recorded in acetonitrile for all complexes and for 1:100 complex/3,5-DTBC mixtures. The base peak at m/z = 588.19 (100%) observed in the mass spectra of **1** and **2** can be assigned to the cationic species $[Ni_2(L^1)_2(NCS)]^+$ (Figure S6, Supporting Information) and $[Ni_2(L^2)_2(NCS)]^+$. The base peak at m/z = 617.35 for **3** is ascribed similarly to the cationic species $[Ni_2(L^3)_2(NCS)]^+$ (Figure S7, Supporting Information). After addition of 3,5-DTBC to the complex solution, new peaks are detected by ESI-MS. Accordingly, the spectra show peaks at m/z = 750.40 for **1** (Figure S8, Supporting Information) and **2**, and 779.49 for **3** (Figure S9, Supporting Information), which can be assigned to the cationic species **A** depicted in Scheme 2. It thus appears that di-nickel(II) species are maintained in solution, although they are obtained from noncompartmental, mononucleating ligands (in contrast to all model complexes published earlier); moreover, these dinuclear units are capable of binding 3,5-DTBC, which allows its metal-mediated oxidation to 3,5-DTBQ.

The cyclic voltammograms of **1**−**3** in acetonitrile at room temperature all display an irreversible reductive responses at E_{pc} = −1.17 V (Figure S10, Supporting Information), which is attributed to the Ni^{II}/Ni^{I} couple. The nonappearance of oxidation peak suggests significant changes in the coordination sphere of the nickel(I) center. Spectro-electrochemical studies are required to analyze further the nature of the species generated electrochemically.

The X-band EPR spectra of 10^{-3} M acetonitrile solutions of the different complexes with added 3,5-DTBC, recorded at 77 K, are dominated by an isotropic signal around g_{iso} = 2.00 (for instance, for complex **1**, g_{iso} = 1.995; see Figure 9), with a peak-to-peak line width of ca. 40 G. The g value of the signal is closed to 2.0023 (value for a free electron[51]), a value that is characteristic for organic radicals, such as a phenoxyl-type radical.[52] Actually, the EPR feature obtained in the present study is comparable to that observed recently for a di-Ni^{II}-phenoxyl radical complex from a mononucleating tridentate N,O,O-ligand.[53] It thus appears that the di-nickel coordination compounds **1**−**3** are capable of oxidizing 3,5-DTBC to 3,5-DTBQ,

Scheme 2. Probable Structure of Complex−Substrate Intermediates According to ESI-MS Measurements

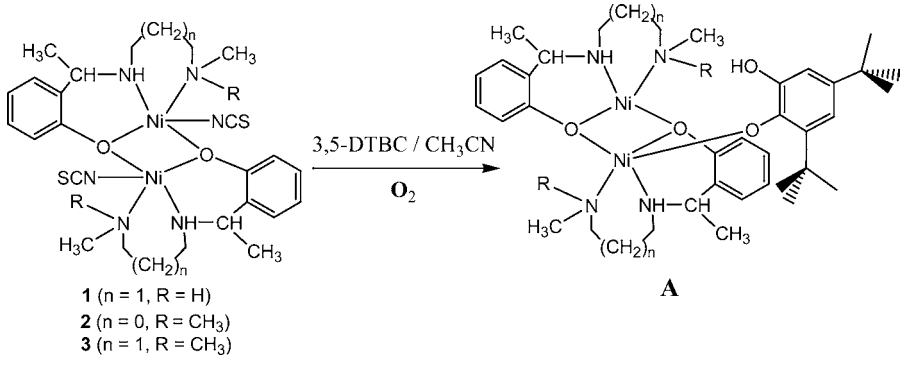

dx.doi.org/10.1021/ic202748m | Inorg. Chem. 2012, 51, 7993−8001

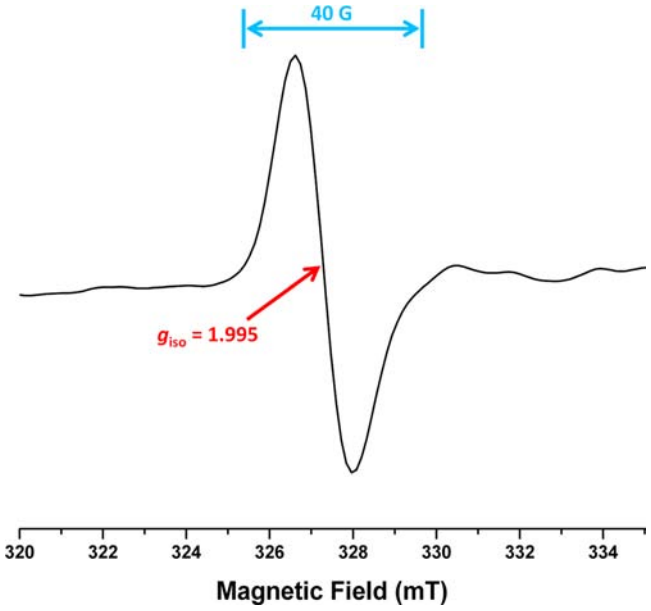

Figure 9. EPR spectrum of an acetonitrile solution of **1**(10^{-3} M) after addition of 3,5-DTBC, recorded at 77K. Microwave frequency: 9.14 GHz.

through a radical pathway, as also proposed for copper-based model complexes.[9]

CONCLUSIONS

The reaction of the tridentate reduced Schiff-base ligands, HL^1, HL^2, and HL^3 with nickel(II) thiocyanate afforded three double phenoxido-bridged dinuclear nickel(II) coordination compounds **1**−**3**. The coordination environment of the antiferromagnetically coupled nickel(II) ions in all three complexes is square pyramidal but with different degrees of distortion toward a trigonal bipyramid. To the best of our knowledge, such a dinuclear core of penta-coordinated nickel(II) ions connected by two phenoxido bridges donors is unprecedented with tridentate Schiff-base ligands. The reduction of the rigid azomethine (—CH═N—) fragment of the Schiff base to the less-constrained —CH_2—NH— moiety seems to stabilize the coordination geometries observed in **1**−**3**. This particular arrangement favors relatively strong antiferromagnetic interactions within the dinuclear entities, simulated with coupling constants of J = −23.32, −35.45, and −34.02 cm^3 K mol^{-1} for **1**, **2**, and **3**, respectively. All three complexes show catecholase activity of different magnitude, which apparently arises from the ring size of the diamine fragment of the ligands and the distortion of penta-coordination geometry; the six-membered chelate rings enhance the catecholase activity while a distortion toward the trigonal-bipyramidal geometry impede the catalytic activity. Mechanistic investigations of the catalytic behaviors of these nickel(II) complexes by electrospray ionization mass (ESI-MS positive) and EPR spectroscopy indicate that, similarly to the copper(II) analogues, the participation of metal centers through a nickel(II)/nickel(I) redox process is responsible for the oxidation of catecholic substrate to quinone.

ASSOCIATED CONTENT

Supporting Information

Additional figures (PDF) and crystallographic data (CIF). This material is available free of charge via the Internet at http://pubs.acs.org.

AUTHOR INFORMATION

Corresponding Authors

*Email: patrick.gamez@qi.ub.es.

*Email: ghosh_59@yahoo.com.

Notes

The authors declare no competing financial interest.

ACKNOWLEDGMENTS

We thank CSIR, Government of India [Senior Research Fellowship to A.B., Sanction No. 09/028 (0717)/2008-EMR-I and Junior Research Fellowship to L.K.D., Sanction No.09/028(0805)/2010-EMR-I] and DST FIST for financial support for the X-ray diffraction facility. We also thank the British Engineering and Physical Sciences Research Council (EPSRC) and the University of Reading for funds for the X-Calibur system. We are also thankful to Prof. Tapan Kanti Paine, Indian Association for the Cultivation of Science for EPR measurements. P.G. and G.A. acknowledge the Ministerio de Ciencia e Innovación of Spain (Projects CTQ2011-27929-C02-01, P.G., and CTQ2009-06959, G.A.) and the support of COST Action CM1003.

REFERENCES

(1) Crichton, R. H. In *Biological Inorganic Chemistry: A New Introduction to Molecular Structure and Function*, 2nd ed.; Elsevier Science: Oxford, 2012.
(2) Friedle, S.; Reisner, E.; Lippard, S. J. *Chem. Soc. Rev.* **2010**, *39*, 2768−2779.
(3) Bruijnincx, P. C. A.; van Koten, G.; Klein Gebbink, R. J. M. *Chem. Soc. Rev.* **2008**, *37*, 2716−2744.
(4) Chan, S. I.; Yu, S. S.-F. *Acc. Chem. Res.* **2008**, *41*, 969−979.
(5) Hage, R.; Lienke, A. *Angew. Chem.* **2006**, *118*, 212−229.
(6) Duran, N.; Esposito, E. *Appl. Catal., B* **2000**, *28*, 83−99.
(7) Que, L.; Tolman, W. B. *Nature* **2008**, *455*, 333−340.
(8) Koval, I. A.; Belle, C.; Selmeczi, K.; Philouze, C.; Saint-Aman, E.; Schuitema, A. M.; Gamez, P.; Pierre, J. L.; Reedijk, J. J. *Biol. Inorg. Chem.* **2005**, *10*, 739−750.
(9) Koval, I. A.; Gamez, P.; Belle, C.; Selmeczi, K.; Reedijk, J. *Chem. Soc. Rev.* **2006**, *35*, 814−840.
(10) (a) Sreenivasulu, B.; Vetrichelvan, M.; Zhao, F.; Gao, S.; Vittal, J. J. *Eur. J. Inorg. Chem.* **2005**, 4635−4645. (b) Neves, A.; Rossi, L. M.; Bortoluzzi, A. J.; Szpoganicz, B.; Wiezbicki, C.; Schwingel, E.; Haase, W.; Ostrovsky, S. *Inorg. Chem.* **2002**, *41*, 1788−1794. (c) Rey, N. A.; Neves, A.; Bortoluzzi, A. J.; Pich, C. T.; Terenzi, H. *Inorg. Chem.* **2007**, *46*, 348−350.
(11) Bhardwaj, V. K.; Aliaga-Alcalde, N.; Corbella, M.; Hundal, G. *Inorg. Chim. Acta* **2010**, *363*, 97−106.
(12) Banu, K. S.; Chattopadhyay, T.; Banerjee, A.; Mukherjee, M.; Bhattacharya, S.; Patra, G. K.; Zangrando, E.; Das, D. *Dalton Trans.* **2009**, 8755−8764.
(13) (a) Guha, A.; Banu, K. S.; Banerjee, A.; Ghosh, T.; Bhattacharya, S.; Zangrando, E.; Das, D. *J. Mol. Cat. A: Chemical* **2011**, *338*, 51−57. (b) Triller, M. U.; Pursche, D.; Hsieh, W.-Y.; Pecoraro, V. L.; Rompel, A.; Krebs, B. *Inorg. Chem.* **2003**, *42*, 6274−6283.
(14) Majumder, A.; Goswami, S.; Batten, S. R.; Fallah, M. S. E.; Ribas, J.; Mitra, S. *Inorg. Chim. Acta* **2006**, *359*, 2375−2382.
(15) Bharathi, K. S.; Sreedaran, S.; Rahiman, A. K.; Rajesh, K.; Narayanan, V. *Polyhedron* **2007**, *26*, 3993−4002.
(16) Chattopadhyay, T.; Mukherjee, M.; Mondal, A.; Maiti, P.; Banerjee, A.; Banu, K. S.; Bhattacharya; Roy, S. B.; Chattopadhyay, D. J.; Mondal, T. K.; Nethaji, M.; Zangrando, E.; Das, D. *Inorg. Chem.* **2010**, *49*, 3121−3129.
(17) Nirmala, G.; Rahiman, A. K.; Sreedaran, S.; Jegadeesh, R.; Raaman, N.; Narayanan, V. *J. Mol. Struct.* **2011**, *989*, 91−100.
(18) Das, S.; Maiti, P.; Ghosh, T.; Zangrando, E.; Das, D. *Inorg. Chem. Commun.* **2012**, *15*, 266−268.

(19) (a) Biswas, A.; Drew, M. G. B.; Ghosh, A. *Polyhedron* **2010**, *29*, 1029−1034. (b) Ganguly, R.; Sreenivasulu, B.; Vittal, J. J. *Coord. Chem. Rev.* **2008**, *252*, 1027−1050.
(20) Biswas, A.; Drew, M. G. B.; Gómez-García, C. J.; Ghosh, A. *Inorg. Chem.* **2010**, *49*, 8155−8163.
(21) Biswas, A.; Drew, M. G. B.; Ribas, J.; Diaz, C.; Ghosh, A. *Eur. J. Inorg. Chem.* **2011**, 2405−2412.
(22) Biswas, A.; Saha, R.; Ghosh, A. *CrystEngComm* **2011**, *13*, 5342−5347.
(23) (a) Biswas, A.; Drew, M. G. B.; Song, Y.; Ghosh, A. *Inorg. Chim. Acta* **2011**, *376*, 422−427. (b) Biswas, A.; Drew, M. G. B.; Ribas, J.; Diaz, C.; Ghosh, A. *Inorg. Chim. Acta* **2011**, *379*, 28−33.
(24) (a) Mandal, S.; Balamurugan, V.; Lloret, F.; Mukherjee, R. *Inorg. Chem.* **2009**, *48*, 7544−7556. (b) Ren, Y. W.; Lu, J. X.; Cai, B. W.; Shi, D. B.; Jiang, H. F.; Chen, J.; Zheng, D.; Liu, B. *Dalton Trans.* **2011**, *40*, 1372−1381.
(25) (a) Banerjee, A.; Guha, A.; Maiti, P.; Goswami, S.; Chattopadhyay, T.; Mondal, T. K.; Bhattacharya, S.; Zangrando, E.; Das, D. *Transition Met. Chem.* **2011**, *36*, 829−839.
(26) Mukherjee, P.; Drew, M. G. B.; Gómez-García, C. J.; Ghosh, A. *Inorg. Chem.* **2009**, *48*, 5848−5860.
(27) Kahn, O. In *Molecular Magnetism*; VCH: New York, 1993.
(28) *CrysAlis*; Oxford Diffraction Ltd.: Abingdon, U.K., 2006.
(29) Sheldrick, G. M. Shelxs97 and Shelxl97, Programs for Crystallographic Solution and Refinement. *Acta Crystallogr.Sect. A* **2008**, *64*, 112−122.
(30) *ABSPACK Program for Absorption Corrections*, Oxford Diffraction: Abingdon, U.K., 2007.
(31) Biswas, C.; Drew, M. G. B.; Ruiz, E.; Estrader, M.; Diaz, C.; Ghosh, A. *Dalton Trans.* **2010**, *39*, 7474−7484.
(32) Mukherjee, P.; Biswas, C.; Drew, M. G. B.; Ghosh, A. *Polyhedron* **2007**, *26*, 3121−3128.
(33) Boge, E. M.; Freyberg, D. P.; Kokot, E.; Mockler, G. M.; Sinn, E. *Inorg. Chem.* **1977**, *16*, 1655−1660.
(34) Addison, A. W.; Rao, T. N.; Reedjik, J.; van Rijn, J.; Verschoor, C. G. *J. Chem. Soc., Dalton Trans.* **1984**, 1349−1356.
(35) (a) Mondal, N.; Mitra, S.; Gramilich, V.; Ghodsi, S. O.; Malik, K. M. A. *Polyhedron* **2001**, *20*, 135−141. (b) Sun, Y.-X. *Acta Crystallogr., Sect. C* **2006**, *62*, m109−m111. (c) Sun, X.-Z.; Shi, J.-S. *Acta Crystallogr., Sect. E* **2006**, *62*, m1130−m1131. (d) You, Z.-L. *Acta Crystallogr. Sect. E* **2005**, *61*, m1963−m1964.
(36) Dey, S. K.; Fallah, M. S. E.; Ribas, J.; Matsushita, J. T.; Gramlich, V.; Mitra, S. *Inorg. Chim. Acta* **2004**, *357*, 1517−1522.
(37) Mukherjee, P.; Drew, M. G. B.; Gómez-García, C. J.; Ghosh, A. *Inorg. Chem.* **2009**, *48*, 4817−4827.
(38) Biswas, R.; Kar, P.; Song, Y.; Ghosh, A. *Dalton Trans.* **2011**, *40*, 5324−5331.
(39) (a) Wu, J.-C.; Li, Y.-Z.; Tang, N.; Tan, M.-Y. *Acta Crystallogr., Sect. E* **2003**, *59*, m494−m496. (b) Nanda, K. K.; Thompson, L. K.; Bridson, J. N.; Nag, K. *J. Chem. Soc., Chem. Commun.* **1994**, 1337−1338. (c) Kong, D.; Mao, J.; Martell, A. E.; Clearfield, A. *Inorg. Chim. Acta* **2002**, *338*, 78−88.
(40) (a) Dey, M.; Rao, C. P.; Saarenketo, P. K.; Rissanen, K. *Inorg. Chem. Commun.* **2002**, *5*, 924−928. (b) Koizumi, S.; Nihei, M.; Oshio, H. *Chem. Lett.* **2003**, *32*, 812−813. (c) Garnovskii, A. D.; Burlov, A. S.; Garnovskii, D. A.; Vasilchenko, I. S.; Antsichkina, A. S.; Sadikov, G. G.; Sousa, A.; Garcia-Vazquez, J. A.; Romero, J.; Duran, M. L.; Sousa-Pedrares, A.; Gomez, C. *Polyhedron* **1999**, *18*, 863−869. (d) Lozan, V.; Lassahn, P.-G.; Zhang, C.; Wu, B.; Janiak, C.; Rheinwald, G.; Lang, H.; Naturforsch., Z. B. *Chem. Sci.* **2003**, *58*, 1152−1164. (e) Tai, X.-S.; Wang, L.-H.; Li, Y.-Z.; Tan, M.-Y. *Z. Kristallogr. New Cryst. Struct.* **2004**, *219*, 407−408.
(41) Kahn, O.; VCH: New York, 1993, p 112.
(42) (a) Halcrow, M. A.; Sun, J.-S.; Huffman, J. C.; Christou, G. *Inorg. Chem.* **1995**, *34*, 4167−4177. (b) Biswas, R.; Giri, S.; Saha, S.-K.; Ghosh, A. *Eur. J. Inorg. Chem.* **2012**, 2916−2927.
(43) Sadhukhan, D.; Ray, A.; Pilet, G.; Rizzoli, C.; Rosair, G.; Gómez-García, C. J.; Signorella, S.; Bellu, S.; Mitra, S. *Inorg. Chem.* **2011**, *50*, 8326−8339.
(44) Nanda, K. K.; Das, R.; Thompson, L. K.; Venkatsubramanian, K.; Paul, P.; Nag, K. *Inorg. Chem.* **1994**, *33*, 1188−1193.
(45) Nanda, K. K.; Thompson, L. K.; Bridson, J. N.; Nag, K. *J. Chem. Soc., Chem. Commun.* **1994**, 1337−1338.
(46) Mukherjee, J.; Mukherjee, R. *Inorg. Chim. Acta* **2002**, *337*, 429−438.
(47) Banu, K. S.; Chattopadhyay, T.; Banerjee, A.; Bhattacharya, S.; Suresh, E.; Nethaji, M.; Zangrando, E.; Das, D. *Inorg. Chem.* **2008**, *47*, 7083−7093.
(48) Banu, K. S.; Chattopadhyay, T.; Banerjee, A.; Bhattacharya, S.; Zangrando, E.; Das, D. *J. Mol. Catal. A: Chem.* **2009**, *310*, 34−41.
(49) Banerjee, A.; Singh, R.; Colacio, E.; Rajak, K. K. *Eur. J. Inorg. Chem.* **2009**, 277−284.
(50) Smith, S. J.; Noble, C. J.; Palmer, R. C.; Hanson, G. R.; Schenk, G.; Gahan, L. R.; Riley, M. J. *J. Biol. Inorg. Chem.* **2008**, *13*, 499−510.
(51) Rieger, P. H. In *Electron Spin Resonance: Analysis and Interpretation*; Royal Society of Chemistry: Cambridge, U.K., 2007.
(52) Wanke, R.; Benisvy, L.; Kuznetsov, M. L.; da Silva, M. F. C. G.; Pombeiro, A. J. L. *Chem.—Eur. J.* **2011**, *17*, 11882−11892.
(53) Benisvy, L.; Wanke, R.; da Silva, M. F. C. G.; Pombeiro, A. J. L. *Eur. J. Inorg. Chem.* **2011**, 2791−2796.

NOTE ADDED AFTER ASAP PUBLICATION

This paper was published on the Web on July 3, 2012, with minor errors in the Synopsis and Abstract graphics. The corrected version was reposted on July 10, 2012.